

Synthesis and Comparison of Linear Polymannosides for Direct Binding with *Escherichia coli*

Natalie Hanheiser, Badri Parshad, Tatyana L. Povolotsky,* Vinod Khatri, Katharina Achazi, and Sumati Bhatia*

Here, the synthesis of linear polyglycerols bearing multiple copies of mono and dimannosides (LPG₄₀Man_{0.60} and LPG₄₀(Man α 1,2Man)_{0.60}) is demonstrated. A method based on label-free microscale thermophoresis is optimized to determine the direct binding affinity of multivalent mannosides for *Escherichia coli* (*E. coli*) strain ORN178 that produces the fimbriae protein FimH. It is observed that the LPG₄₀(Man α 1,2Man)_{0.60} exhibits only a modest onefold improvement in binding as compared to LPG₄₀Man_{0.60}. Nevertheless, both the multivalent mannosides display remarkably very low nM binding constant (K_d) in contrast to the high μ M K_d of the single α -D-methylmannoside for intact *E. coli* ORN178 particles. Furthermore, in an adhesion-inhibition assay, both multivalent mannosides show 50% inhibition of bacteria adhesion to the HT-29 colon cells at low μ M concentrations.


1. Introduction

Bacterial infections stand as a significant global health concern, particularly for vulnerable individuals such as hospitalized patients and those with compromised immune systems. Among

N. Hanheiser, B. Parshad, T. L. Povolotsky, V. Khatri, K. Achazi, S. Bhatia
 Institute for Chemistry and Biochemistry
 Free University of Berlin
 14195 Berlin, Germany
 E-mail: tatyana.povolotsky@fu-berlin.de; sumati.bhatia@swansea.ac.uk

B. Parshad
 Wellman Center for Photomedicine
 Massachusetts General Hospital
 Harvard Medical School
 Boston, MA 02129, USA

V. Khatri
 Department of Chemistry
 T.D.L. Government College for Women
 Murthal, Haryana 131027, India
 S. Bhatia
 Department of Chemistry
 Faculty of Science and Engineering
 Swansea University
 Swansea SA2 8PP, UK

 The ORCID identification number(s) for the author(s) of this article can be found under <https://doi.org/10.1002/macp.202300339>

© 2023 The Authors. Macromolecular Chemistry and Physics published by Wiley-VCH GmbH. This is an open access article under the terms of the Creative Commons Attribution License, which permits use, distribution and reproduction in any medium, provided the original work is properly cited.

DOI: 10.1002/macp.202300339

these infections, *Escherichia coli*, a gram-negative and facultatively anaerobic bacterium poses a noteworthy threat and is responsible for many afflictions including enteritis, septicemia, diarrhea, foodborne illnesses, and urinary tract infections.^[1–6] Over 80% of urinary tract infections are caused by *E. coli*.^[7] The adhesion of *E. coli* to the host cell surface is mediated by type 1 fimbriae, which contains a mannose-specific adhesin known as FimH. *E. coli* can bind to the uroplakin 1 (UPK1a) present on the luminal membrane of urothelial cells. UPK1a displays terminal mannose residues, which can be specifically recognized by the FimH receptor of *E. coli*.^[8] The specific binding mechanism of mannose

and the carbohydrate recognition domain (CRD) of the FimH receptor was previously investigated by Hultgren et al.^[9] They observed that the mannose was submerged in the negatively charged binding pocket of the CRD. Furthermore, every hydroxy group of the mannose ring formed direct and indirect water-mediated hydrogen bonds in the CRD with the FimH binding site.

The infection cycle of *E. coli* starts with the adhesion of the bacteria to the urinary tract cells followed by the invasion of *E. coli* to the bladder cells which enables the bacteria to persist and multiply. The bacterial colonization on the host cell surface then causes the inflammation of the tissue.^[10] Therefore, much effort has been made to understand the *E. coli* binding via FimH glycoproteins and the development of mannoside-based glyco-inhibitors for bacteria.^[11,12] For example, tetrameric mannosylated dendrimers by Roy and co-workers showed low K_d of 0.45 nM as compared to single α -D-methylmannoside with K_d of 2200 nM with FimH adhesin via surface plasmon resonance (SPR).^[13] Similarly, Lee and co-workers studied how different designs of multivalent mannosides enhanced the binding avidity toward mannose-specific adhesin on *E. coli* K-12 cells.^[14] All inhibitors were based on a neoglycoprotein incorporating O-mannosides. The design of multivalent mannosides varied in the form of the linking arm structure and the degree of mannosylation. Mono, di, and trivalent cluster ligands, as well as dendrimeric ligands, were assessed in a competitive binding assay. The results demonstrated a decrease in the IC₅₀ as the degree of mannosylation increased. Highly mannosylated neoglycoproteins with the longest spacer length of 14 showed sub-nM IC₅₀ values for the *E. coli* K-12 adhesion inhibition. Also, mannose functionalized cyclodextrin vesicles (CDVs) by Haag and

co-workers were efficient in detaching *E. coli* ORN178 from the human uroepithelial cell line RT-4.^[15]

In addition to α -D-mannoside, both Man α -1,2Man and Man α -1,3Man epitopes were screened by Krammer and co-workers for their adhesion to FimH in an enzyme-linked lectin sorbent assay (ELLSA). The mono and dimannoside epitopes showed IC₅₀ values in the micromolar range for the adhesion inhibition of FimH in the ELLSA.^[16]

No effective methods to determine the direct binding affinity of multivalent systems for full bacteria particles in solution have been reported yet. The development of such methods would be invaluable for investigating the direct interactions of multivalent scaffolds with large pathogens, like bacteria, and facilitating direct, efficient screening for inhibitors in solution. In this work, the aminopentyl derivative of α -D-mannoside and Man α -1,2Man dimannoside were synthesized by modified procedures. Subsequently, these derivatives were conjugated to the biocompatible linear polyglycerol (LPG) polymer backbones to afford medium-functionalized glycopolymers. Next, the label-free microscale thermophoresis (MST) based method was optimized to determine the apparent binding constants ($K_{d,app}$) of linear polymers bearing multiple copies of α -D-monomannosides and Man α -1,2Man dimannosides against intact *E. coli* ORN178. It is worth noting that so far MST measurements have been mostly applied to isolated proteins^[15] and whole virus particles^[17] and this is the first work that employed the whole intact *E. coli* ORN178 bacterial organism in successfully measuring binding affinity with the MST method.

The multivalent LPG₄₀(Man α 1,2Man)_{0,60} resulted in a very low nM binder of *E. coli* ORN178 with a remarkably high almost 10⁵ times stronger than α -D-methylmannoside. Subsequently, in vitro assays were conducted to evaluate the effectiveness in preventing the adhesion of *E. coli* to the host cell surface of human colon cells (HT29) demonstrating low μ M inhibition efficiency of multivalent mono and dimannosides.

2. Results and Discussion

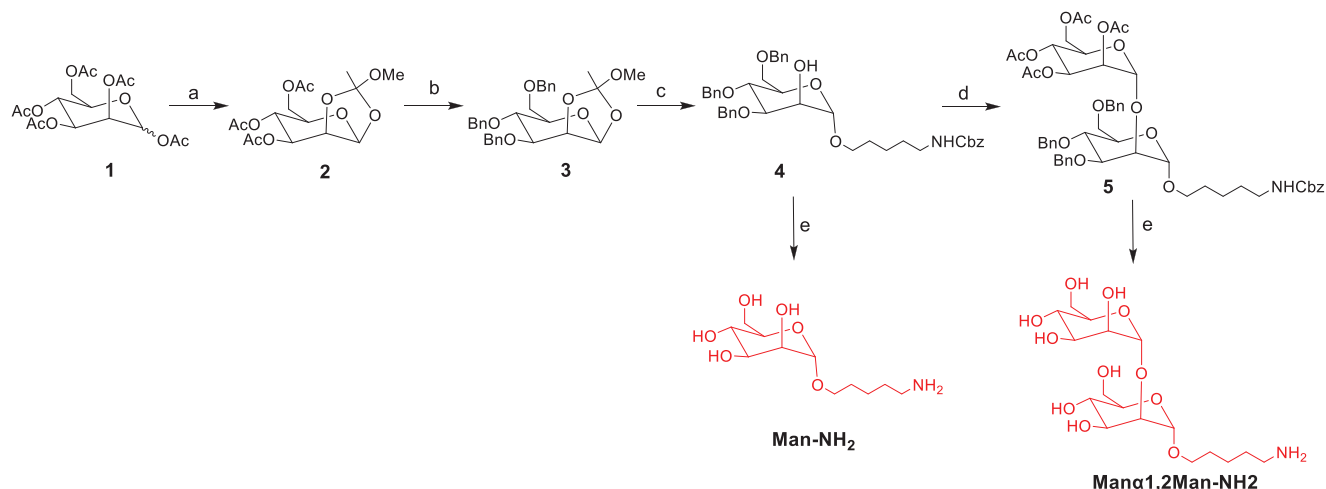
2.1. Design, Synthesis, and Characterization of Monovalent Ligands

With the aim to develop multivalent architectures for inhibiting bacterial adhesion to the host cells, α -D-mannoside (Man) and di-mannoside (Man α 1,2Man) ligands were selected that target the FimH receptor of *E. Coli*. The aminopentyl derivatives of α -D-mannose (Man-NH₂) and di-mannose (Man α 1,2Man-NH₂) were utilized to couple with carboxylic acid groups of polymers to obtain the polymannosides. Both Man-NH₂ and Man α 1,2Man-NH₂ were synthesized in multiple steps from the commercially available mannoside pentaacetate by modifying the procedure reported earlier.^[18,19] Mannoside pentaacetate was first treated with HBr/AcOH followed by treatment with 2,6-lutidine to obtain cyclic orthoacetate derivative 2 which is confirmed by observance of -OMe peak at δ 3.26 in ¹H NMR. Subsequent deacetylation and then benzylation using benzyl chloride and potassium hydroxide afforded the benzyl analog 3. The disappearance of three singlets at δ 2.10, 2.05, and 2.03 ppm for -OAc and the appearance of multiplet in the range of δ 7.41–7.22 ppm confirm the formation of compound 3. A flexible aminopentyl chain was then introduced

to obtain the compound 4 which serves as a common intermediate for the synthesis of both Man-NH₂ and Man α 1,2Man-NH₂. O-glycosylation of compound 4 with compound S1 (Supporting Information) in the presence of trimethylsilyl triflate yielded the protected di-mannoside 5, established from the observance of four singlets at δ 2.13, 2.11, 2.03, and 2.02 ppm in ¹H NMR. Hydrolysis of compounds 4 and 5 in the presence of NaOMe followed by debenylation using H₂/Pd yielded the compounds Man-NH₂ and Man α 1,2Man-NH₂, respectively (Scheme 1). In high-resolution mass spectrometry (HRMS) analysis of the synthesized compounds, peaks corresponding to [M+H]⁺ and/or [M+Na]⁺ were observed, which were in accordance with their respective molecular formulas.

2.2. Design, Synthesis, and Characterization of Multivalent Glycopolymers

We selected 40 kDa linear polyglycerol (LPG₄₀OH) for the multivalent display of different ligands. Glycosylated polymers with a moderate degree of functionalization have previously demonstrated their ability to provide a sufficient number of sugar residues for lectin and pathogen binding. Typically, a significant jump in binding is observed when the sugar ratio on a polymer reaches above 30%. For example, Papp et al. reported 10% mannose on hyperbranched polyglycerol (hPG) to be weakly active against Concanavalin A lectin.^[20] Bacer et al. observed an effective inhibition of DC-SIGN and gp120 when the mannose residues on the polymer backbone were increased from 25% to 50%.^[21] Our previous report revealed that the optimal ligand density of carbohydrate ligands on the LPG scaffold for targeting hemagglutinin (HA) glycoproteins on an influenza A virus surface fell within 40–70%.^[22,23] Therefore, we selected LPG₄₀OH with a moderate degree of 60% mannosides or dimannosides to serve as multivalent ligands for targeting the FimH proteins in *E. coli*. Both the glycosylated polymers were synthesized in three steps. First, LPG with 60% alkyne (LPG₄₀Alkyne_{0,60}) functionalization was prepared by the reaction of LPG₄₀OH with propargyl bromide. The formation of LPG₄₀Alkyne_{0,60} and the degree of alkylation/propargylation were determined by nuclear magnetic resonance (NMR) (Figure S11, Supporting Information). The appearance of terminal alkyne (\equiv CH) protons at δ 2.49 and methylene ($-\text{OCH}_2-\text{C}\equiv$) at δ 4.17 confirmed the formation of LPG₄₀Alkyne_{0,60}. The degree of alkylation was calculated by comparing the number of protons of LPG backbone with alkyne group protons where the integration of LPG backbone protons at δ 3.65 for five protons (one unit) automatically integrated the peaks at δ 2.49 (\equiv CH) for 0.6 protons and δ 4.17 ($-\text{OCH}_2-\text{C}\equiv$) for 1.2 protons, thus confirming the degree of alkylation is equal to 60%. LPG₄₀Alkyne_{0,60} was then reacted with ethyl 3-azidopropanoate using copper-catalyzed azide-alkyne cycloaddition (CuAAC) click reaction followed by basic hydrolysis in the presence of NaOH to afford LPG₄₀Acid_{0,60} polymer in high yield. The formation of LPG₄₀Acid_{0,60} was confirmed by the disappearance of the terminal alkyne peak at δ 2.49 and the appearance of a triazole characteristic peak at δ 8.03. In the final step, LPG₄₀Acid_{0,60} was coupled with Man-NH₂ and Man α 1,2Man-NH₂ to get the desired LPG₄₀Man_{0,60} and LPG₄₀(Man α 1,2Man)_{0,60} polymers, respectively (Scheme 2). A



Scheme 1. Synthesis of Man-NH₂ and Man α 1,2Man-NH₂. Reagent and conditions: a) i) 33% HBr/AcOH, dry DCM, rt, 2 h, ii) 2,6-lutidine, dry MeOH, dry DCM, rt, 16 h; b) KOH, BnCl, dry THF, 70 °C, 16 h; c) i) BF₃·Et₂O, dry DCM, benzyl *N*-(5-hydroxypentyl)carbamate, rt, 2 h, ii) NaOMe, MeOH, rt, 4 h; d) TMSOTf, compound S1, dry DCM, rt, 1 h; e) i) NaOMe, MeOH, rt, 2 h, ii) H₂, Pd/C, CF₃CH₂OH, H₂O, HCOOH, rt, 24 h.

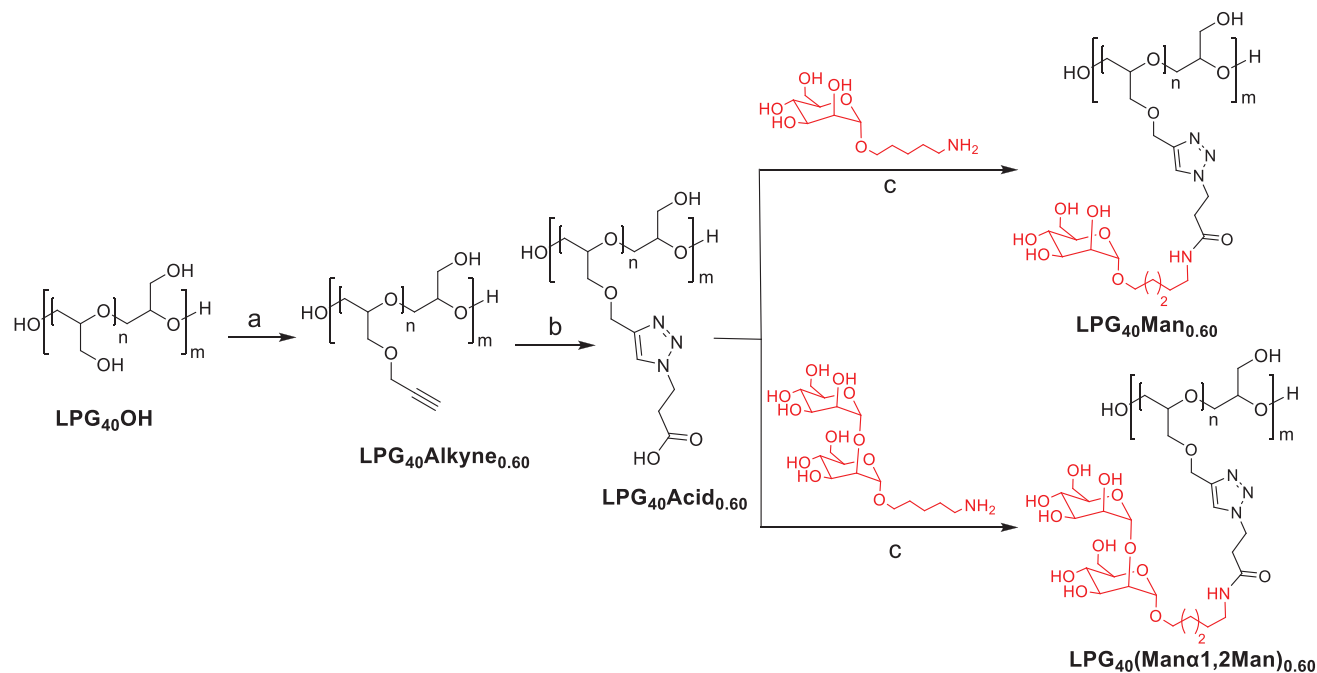
large excess of Man-NH₂ and Man α 1,2Man-NH₂ was utilized to make sure that each acid group reacted to give complete functionalization of 60%, which was also confirmed by the integration of ¹H NMR peaks in the region between \approx 4 and δ 1.08 for aminopentyl mannose units. Integration of mannose and pentyl group protons and their comparison with triazole protons also confirmed the complete 60% functionalization.

The size distribution profiles of the synthesized glycopolymers were analyzed using dynamic light scattering (DLS) in DI water (Table 1 and Figure 1). The conjugation of mannoses on LPG led to an almost 50% increase in the hydrodynamic shell of the

glycopolymer. The hydrodynamic diameter (D_h) of the mannose-conjugated LPG was observed to be higher than that of the LPG itself. This is due to their increased aqueous solvation shell after functionalization with the hydrophilic sugar residues.

2.3. Determination of Binding Affinity of Polyglycerol Mannosides to Intact Bacteria

We selected label-free MST for the quantitative determination of direct binding affinities of polymannosides LPG₄₀Man_{0,60} and



Scheme 2. Synthesis of mannose-functionalized glycopolymers. Reagent and conditions: a) Propargyl bromide, NaH, DMF, rt, 24 h; b) i) ethyl 3-azidopropanoate, CuSO₄·5H₂O, sodium ascorbate, DMF:H₂O, 45 °C, ii) 2 N aq. NaOH, rt, 3 h; c) EDC.HCl, HOBT, DIPEA, DMF:H₂O, 50 °C, 48 h.

Table 1. Characterization of synthesized mannosylated LPGs.

Compound	LPG _{MW} Man _{DF}	DF [%]	Ligands per polymer	D _h [nm]	PDI	Man/nm ²
LPG ₄₀ OH		0	0	7.61 ± 1.56	0.28	–
LPG ₄₀ Man _{0.60}		60	324	11.23 ± 3.65	0.32	0.82
LPG ₄₀ (Man α 1,2Man) _{0.60}		60	324	11.12 ± 5.57	1.00	0.83

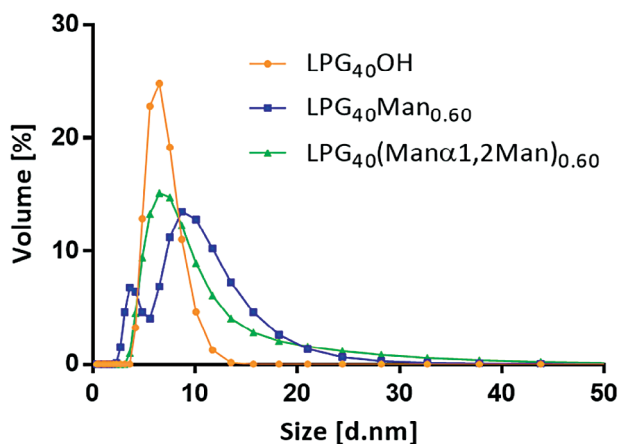


Figure 1. Size analysis of linear polyglycerol-based inhibitors by DLS. The volume distributions of linear polyglycerol (LPG₄₀OH), and linear polyglycerol mannosides (LPG₄₀Man_{0.60} and LPG₄₀(Man α 1,2Man)_{0.60}) diluted in DI water at 25 °C.

LPG₄₀(Man α 1,2Man)_{0.60}, unfunctionalized control linear polyglycerol LPG₄₀OH and α -D-methylmannopyranoside (MeMan) with intact *E. coli* ORN 178. In label-free MST, the intrinsic fluorescence of proteins was harnessed to investigate how molecules move when subjected to a temperature gradient.^[24] Thus, in this case, *E. coli* could be used without any labeling procedures and prepared for the measurements as discussed above. The apparent binding constant (K_d^{app}) was then determined by assessing alterations in the thermophoretic behavior induced by the binding of the multivalent compounds to the bacteria particles.^[25] This method offers a precise and resource-efficient means of characterizing molecular interactions. The results are shown in Table 2 and Figure 2. For the LPG₄₀Man_{0.60} and LPG₄₀(Man α 1,2Man)_{0.60}, the $K_d^{\text{app}}_{\text{poly}}$ was 29.67 (9.6107 nM mannose) and 3.14 μ M (1.0182 nM mannose), respectively. The single MeMan showed K_d^{app} as 918.950 μ M (Figure 2) and no binding was observed

Table 2. A summary of apparent binding constants (K_d^{app}) is shown together with the confidence values (\pm), indicating with 68% certainty the range in which K_d falls.

Compound	$K_d^{\text{app}}_{\text{Man}}$ [nM]	$K_d^{\text{app}}_{\text{poly}}$ [nM]
MeMan	918950 ± 862490	–
LPG ₄₀ OH	ND*	–
LPG ₄₀ Man _{0.60}	9.610 ± 5.9065	0.029
LPG ₄₀ (Man α 1,2Man) _{0.60}	1.018 ± 0.85965	0.003

*not detected with $n = 3$; Man: mannose ligand, Poly: Polymer, $n \geq 5$, where n is the number of biological repeats.

with the control LPG₄₀OH (Figure S20, Supporting Information). Thus, the optimized label-free MST method allowed the screening of different compounds against intact bacteria in solution. With multivalent mannosides, we observed up to a fivefold increase in binding affinity as compared to the monovalent MeMan ligand. The binding affinity of Mannose and Man α 1,2Man for the FimH protein was earlier measured as 942 nM^[16] and 1.672 μ M^[26] respectively, using isothermal titration calorimetry (ITC). Our observation of K_d^{app} value for MeMan in the high μ M range can be attributed to using the whole *E. coli* ORN178 organism with many FimH proteins are expressed when in planktonic form.

2.4. Adhesion-Inhibition Assay

We utilized the adhesion-inhibition assay to determine at which concentration the multivalent scaffolds with different mannosides attached can prevent the adhesion of *E. coli* to HT-29 cells. LPG₄₀OH was used as a negative control. Among the series of tested inhibitors, the mannosylated compounds showed an inhibition of bacterial adhesion to HT29 cells (Figure 3). Both the multivalent LPG₄₀Man_{0.60}, LPG₄₀(Man α 1,2Man)_{0.60}, decreased 50% of the bacterial adhesion to the HT-29 cells at

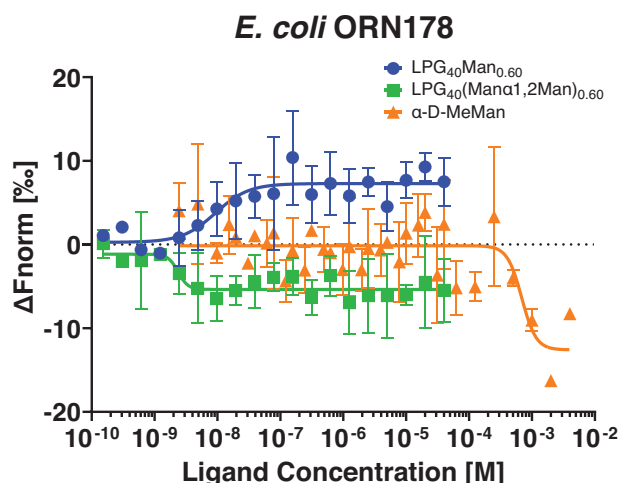


Figure 2. Bacteria binding assay of LPG₄₀Man_{0.60}, LPG₄₀(Man α 1,2Man)_{0.60}, and α -D-MeMan with whole *Escherichia coli* ORN178 bacteria cells. Microscale thermophoresis: Change in fluorescence ΔF_{norm} upon binding of LPG₄₀Man_{0.60}, LPG₄₀(Man α 1,2Man)_{0.60}, and α -D-MeMan at different concentrations to autofluorescent bacteria at the steady state. The single α -D-MeMan molecule served as control. The MST plot for the control polymer LPG₄₀OH without any mannose residues is provided in Figure S20, Supporting Information. Determined binding constants are summarized in Table 2. Plotted is the mean of at least five or more independent measurements ($n \geq 5$) with SEM.

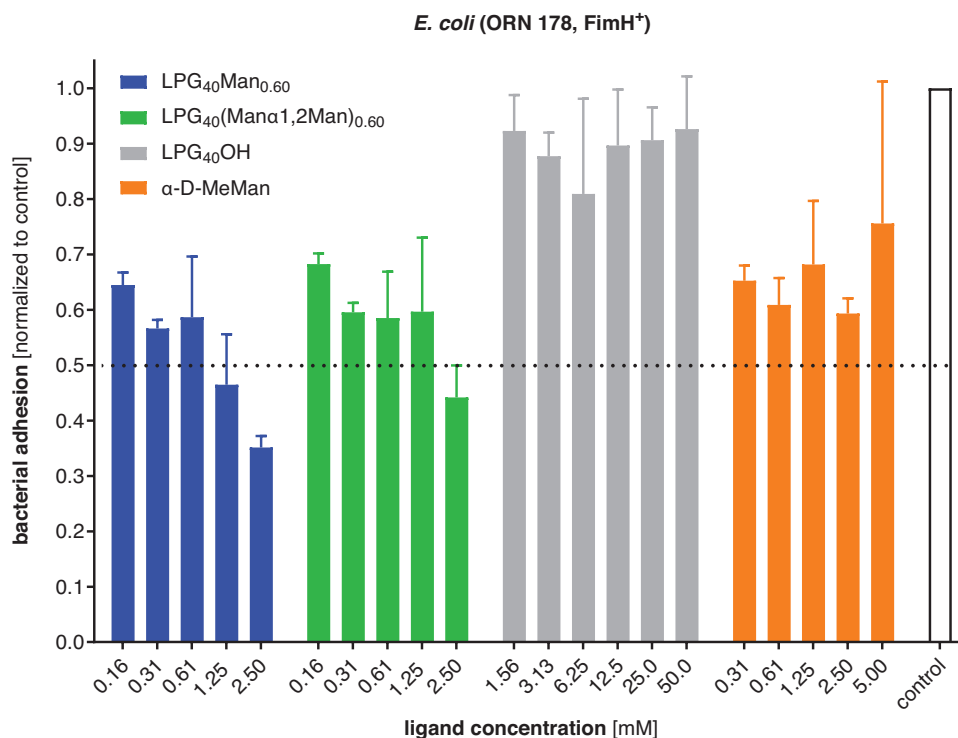


Figure 3. Adhesion-inhibition assay: Inhibition of *Escherichia coli* ORN178 bacterial binding on HT-29 cells obtained by application of mannosylated linear polyglycerol (LPG₄₀Man_{0.60} & LPG₄₀(Man α 1,2Man)_{0.60}), mannose lacking linear polyglycerol (LPG₄₀OH) and the single mannose ligand (α -D-MeMan). The binding was normalized to the control without inhibitor treatment.

low mM mannose concentrations of 1.25 mM (3.8 μ M polymer) for LPG₄₀Man_{0.60} and 2.50 mM (7.7 μ M polymer) for LPG₄₀(Man α 1,2Man)_{0.60} (Figure 3). For the α -D-MeMan, no adhesion inhibition of *E. coli* ORN178 to HT-29 cells below 50% was not observed until the highest concentration was tested (5.00 mM). These results are in agreement with the trend in binding affinities as measured by the MST, where the LPG₄₀Man_{0.60} and LPG₄₀(Man α 1,2Man)_{0.60}, showed up to fivefold higher binding affinities than the α -D-MeMan (Table 2).

3. Conclusion

We here provided a synthetic approach for the preparation of aminated mono and dimannoside derivatives and their conjugation with the LPG backbone. The similar-sized multivalent mono and dimannosides based on LPG scaffolds with similar chemical linkage and glycan density were prepared and compared for their binding with *E. coli* ORN 178. The label-free MST-based method was applied to determine the binding affinities of multivalent scaffolds against intact bacteria particles. A comparison of mono and dimannoside glycoconjugates revealed a small preference for dimannoside polyglycerol for the *E. coli* ORN 178 binding. The LPG-based LPG₄₀(Man α 1,2Man)_{0.60} was the most potent candidate for *E. coli* ORN 178 with a K_d of 3.14 μ M (1.0182 nm dimannoside), and it was approximately sixfold more active than the monovalent MeMan (K_d = 918.95 μ M). The synthetic approach developed for the synthesis of multivalent glycosides, along with the optimized method for assessing binding

constants against *E. coli*, can be possibly applied to other bacterial strains as well and thus holds a significant promise for advancing the field of multivalent antimicrobials, particularly in combating large micrometer-sized pathogens.

4. Experimental Section

Materials: All the solvents and reagents used in the study were analytical grade and were procured from commercial suppliers. These materials were used without further distillation or purification. The solvents, such as hexane, dichloromethane, methanol, ethyl acetate, and tetrahydrofuran, which were used for conduction reactions and column purification, were purchased from VWR chemicals. The starting material, α , β -D-mannose pentaacetate (**1**), was sourced from Biosynth, and HPLC grade α , β -D-methylmannopyranoside was bought from Sigma-Aldrich. Reagents, like HBr/AcOH, 2,6-lutidine, BF₃·Et₂O, and TMSOTf, employed in the synthetic of monovalent ligands, were obtained from Sigma-Aldrich. In the case of small molecules, the progress of the reactions was monitored by thin-layer chromatography (using Merck silica gel 60 F254 pre-coated) and the spots on the TLC were visualized by 5% H₂SO₄/Ethanol and ceric solution staining. Monovalent sugar molecules (compounds **2–5**) were purified by column chromatography, utilizing hexane and ethyl acetate as the eluents. Large polymers were purified by dialyzing against water, using dialysis membranes with a molecular weight cutoff of 10 kDa. Dulbecco's phosphate buffer solution (DPBS, w/o Calcium, w/o Magnesium) (pH = 7.2) was purchased from PAN-Biotech (Cat. No.: P04-36500). Lyso-gen broth (LB) medium (Carl Roth GmbH, Art.-Nr.: X968.2) was used for culturing bacteria. 96-well flat plate transparent for cell culture was purchased from Sarstedt (Sarstedt 96 Flat Transparent Cat. No.: 83.3924). Dulbecco's modified Eagle's medium (DMEM) (Carl Roth GmbH Art.-Nr. 9007.1) + 10% fetal bovine serum (FBS) from Thermo Fisher (Cat. No.:

10270-106) + 1% penicillin-streptomycin (PS) from Sigma-Aldrich (Cat. No.: P433-100 mL). The *E. coli* strain ORN178 positive for FimH (Russell & Orndorff, 1992) was used for all the experiments.^[27] HT-29 cells (DMSZ No.: ACC 299) were cultured in DMEM supplemented with 10% FBS and 1% PS until they were $\approx 70\%$ confluent and then sub-cultured or used for experiments. MST- capillaries were purchased from NanoTemper Technologies GmbH (Cat. No. MO-Z025).

Nuclear Magnetic Resonance, Infrared Spectroscopy, High-Resolution Mass Spectrometry, Gel Permeation Chromatography, and Dynamic Light Scattering Measurements: ^1H and ^{13}C NMR spectra were recorded on Bruker AMX 500 and 125 MHz, respectively, by using residual solvent peak as an internal reference. Chemical shift values were shown on the δ scale while the coupling constant (J) was in Hz. ESI-HRMS was measured on the TSQ 7000 (Finnigan Mat) instrument. The molecular weight distribution (M_n and M_w) of the LPG was determined by using gel permeation chromatography (GPC) from Agilent (Santa Clara, USA) equipped with an Agilent 1100 pump, column, and refractive index detector. Water was used as a mobile phase with a flow rate of 1 mL per minute. The molecular weight of the polymer was calibrated by using pullulan as a standard. Infrared (IR) spectra were recorded with a Nicolet AVATAR 320 FTIR 5 SXC (Thermo Fisher Scientific, Waltham, MA, USA) with a DTGS detector from 4000 to 650 cm^{-1} . The glycopolymers' particle size distribution was analyzed using the Zetasizer (Malvern Zetasizer-Nano ZS, Malvern Instruments Limited, Worcestershire, UK) at a concentration of 5 μm in MilliQ water at a temperature of 25 $^\circ\text{C}$. The system was allowed to equilibrate for 5 s before measurements were taken. Intensity, volume, and number-based size distributions, as well as the PDI values, were recorded.

Microscale Thermophoresis: All samples, containing LPG_{40}OH , $\text{LPG}_{40}\text{Man}_{0.60}$, $\text{LPG}_{40}(\text{Man}\alpha 1,2\text{Man})_{0.60}$, and $\alpha\text{-D-methylmannopyranoside}$ ($\alpha\text{-D-MeMan}$), were adjusted to the following stock concentrations (8 mM for $\alpha\text{-D-MeMan}$ and 160 μM for all other compounds) in MST optimized buffer [50 mM TrisHCl pH 7.4, 150 mM NaCl, 10 mM MgCl_2 , 0.2% Pluronic F-127]: 1:1 serial dilutions with the MST optimized buffer and 1:1 with the bacteria solution, which serves here as a fluorescent binding analyte were prepared. Each solution was filled into Monolith NT.LabelFree Premium Capillaries. MST was measured using the Monolith NT.LabelFree system (NanoTemper Technologies GmbH) at 25 $^\circ\text{C}$ at a wavelength of 275 300 and 350 400 nm and standard settings (MST power = Medium, LED power 20%).

Data from at least five independent measurements were analyzed using the MO.Affinity Analysis software provided by NanoTemper and plotted with GraphPad Prism.10.0.2. The change in fluorescence was expressed as ΔF_{norm} (%) after subtraction of the background.

For the MST measurement, the bacteria solution was prepared as follows. *E. coli* ORN178 bacterial strain was freshly streaked out from frozen stock and single-colony was inoculated into LB-medium (7.00 mL) and allowed to grow to mid-exponential phase (OD_{600} 0.5) at 37 $^\circ\text{C}$ at 250 rpm. The bacteria were washed with DPBS and resuspended in 5 mL of Histofix. After an incubation time of 1 h at room temperature in an Orbital Shaker at 250 rpm. Subsequently, the culture was centrifuged at 3000 rcf for 5 min and the supernatant was discarded. The bacterial pellet was resuspended in DPBS before being centrifuged again. The supernatant was again discarded, and the pellet was resuspended in 3 mL in MST optimized buffer (see above). The resulting culture was diluted to a final concentration of $\text{OD} = 0.1$ and stored on ice. To confirm that the bacteria were fixed, 100 μL of culture was plated on LB agar plates and incubated at 37 $^\circ\text{C}$ overnight (bacteria should not grow).

Adhesion-Inhibition Assay: The adhesion-inhibition assay was adapted from the literature reported by Fessele et al.^[28] and Hartmann et al.^[29] For the assay, HT-29 cells cultured in DMEM ($c = 1.2 \times 10^6$ cells/mL) as described above were added (100 μL /well) to each well of a transparent 96-well cell culture plate. The plate with lid was kept in the incubator at 37 $^\circ\text{C}$ for 24–48 h until they reached confluency. Before the experiment, the healthy morphology of the cells was checked under the microscope. Then, the plate was washed with DPBS (100 μL /well) one time before adding the bacteria solution.

E. coli ORN178 cultured overnight in LB medium (5.00 mL) using an orbital shaker (37 $^\circ\text{C}$ and 125 rpm), were transferred to a falcon tube, and

then centrifuged at room temperature (3 min at 3200 rcf). The bacteria were resuspended in DPBS (5.00 mL) and again centrifuged (3 min at 3200 rcf) and resuspended again in DPBS and adjusted to an OD_{600} of 0.25 to 0.30 using a plate reader (Tecan Austria GmbH, SPARK, REF:30 086 376).

In parallel, serial dilutions of all compounds LPG_{40}OH , $\text{LPG}_{40}\text{Man}_{0.60}$, $\text{LPG}_{40}(\text{Man}\alpha 1,2\text{Man})_{0.60}$, and $\alpha\text{-D-MeMan}$ were prepared in DPBS. Then the inhibitor dilutions and DPBS as control were applied to the plate (50 μL /well) in technical duplicates together with the prepared bacteria solution (50 μL /well). The plate was incubated for 45 min in an orbital shaker (37 $^\circ\text{C}$ and 125 rpm) and then not adhered bacteria were washed off with DPBS buffer twice (100 μL /well). To access the remaining density of bacteria that adhered to the cells, LB medium (100 μL /well) was added to each well, the plate was placed in a plate reader at 37 $^\circ\text{C}$ and the OD_{600} was measured every 15 min for 4 h with shaking for 2 s at 5 Hz before each measurement.

Depending on the potential of the inhibitor to bind to the bacteria and prevent adhesion to the HT-29 cells, more or less bacteria should have remained in each well. As the remaining number of bacteria was too low to access directly, LB medium (100 μL /well) was added to each well and the plate was placed at 37 $^\circ\text{C}$ in a plate reader so that the bacteria could start to grow again. The OD_{600} was measured every 15 min with shaking for 2 s at 5 Hz before each measurement to monitor the increase in the bacteria density that correlates to the number of bacteria that adhered to the HT-29 cells. For analysis, the OD_{600} at 2.5 h was used as here all wells with bacteria solution showed a datable OD_{600} , were in the exponential growth phase, and not already in the saturation.

To access the inhibition potential of the inhibitors, the OD_{600} values for each well at 2.5 h corresponding to the adhered bacteria were normalized to the control wells having bacteria without inhibitors. For data representation, GraphPad Prism.6 was used.

Synthesis of Aminopentyl Mono and Dimannosides (Man-NH_2 and $\text{Man}\alpha 1,2\text{Man-NH}_2$): The aminopentyl derivatives of α -mannoside (Man-NH_2 and $\text{Man}\alpha 1,2\text{Man-NH}_2$) were synthesized in multiple steps as shown in Scheme 1.

Synthesis of Compound 2: To a stirring solution of mannose pentaacetate (**1**) (20 g, 51.24 mmol, 1 eq) in dry DCM (200 mL), 33% HBr in acetic acid (50 mL) was added and the reaction mixture was stirred at rt for 2 h. After completion of the reaction as monitored by TLC, cold water (200 mL) was added, and the organic layer was separated using a separating funnel. The aqueous layer was washed twice with DCM and the combined organic layer was washed with saturated sodium bicarbonate and brine. The organic layer was then dried over Na_2SO_4 and concentrated to yield the anomeric bromide derivative which was used further without purification. Bromo derivative (21 g, 51 mmol, 1 eq) was taken in a mixture of dry DCM and dry methanol (200 mL, 1:1), and to it 2,6-lutidine (21.86 g, 204 mmol, 4 eq) was added. The reaction was stirred at rt for 16 h. The solvent was removed under reduced pressure and the residue obtained was co-evaporated with toluene (2×100 mL). The crude product was redissolved in DCM, washed with brine, dried over anhydrous Na_2SO_4 , and concentrated. The obtained crude product was purified by column chromatography using hexane/ethyl acetate to yield the desired product **2** (15 g, 81%). ^1H NMR (500 MHz, CDCl_3): δ 5.48 (d, 1H, $J = 2.6$ Hz), 5.28 (t, 1H, $J = 9.7$ Hz), 5.13 (dd, 1H, $J = 9.9, 4$ Hz), 4.60 (dd, 1H, $J = 4, 2.6$ Hz), 4.22 (dd, 1H, $J = 12.2, 4.9$ Hz), 4.13 (dd, 1H, $J = 12.1, 2.7$ Hz), 3.69–3.65 (m, 1H), 3.26 (s, 3H), 2.10 (s, 3H), 2.05 (s, 3H), 2.03 (s, 3H), 1.72 (s, 3H). HRMS (ESI): Calculated for $\text{C}_{15}\text{H}_{22}\text{O}_{10}$ $[\text{M}+\text{Na}]^+$ 385.1105, found 385.1109.

Synthesis of Compound 3: To a stirring solution of **2** (5 g, 13.8 mmol, 1 eq) in dry THF (50 mL), benzyl chloride (31.7 mL, 276 mmol, 20 eq) and powdered KOH (15.48 g, 276 mmol, 20 eq) were added, and the reaction mixture was stirred at 70 $^\circ\text{C}$ for 16 h. After completion of the reaction as monitored by TLC, cold water (200 mL) was added, and the reaction mixture was diluted with DCM (200 mL). The organic layer was separated using a separating funnel. The aqueous layer was washed with DCM (2×100 mL) and the combined organic layer was washed with saturated sodium bicarbonate and brine. The organic layer was then dried over anhydrous Na_2SO_4 and concentrated. The obtained crude product was purified by column chromatography using hexane/ethyl acetate to yield the

desired product **3** (5.45 g, 78%). $^1\text{H NMR}$ (500 MHz, CDCl_3): δ 7.41–7.22 (m, 15H), 5.35 (d, 1H, $J = 2.5$ Hz), 4.90 (d, 1H, $J = 10.8$ Hz), 4.78 (q, 2H, $J = 12.2, 2.1$ Hz), 4.64–4.53 (m, 3H), 4.39 (dd, 1H, $J = 3.9, 2.5$ Hz), 3.92 (t, 1H, $J = 9.3$ Hz), 3.77–3.69 (m, 3H), 3.44–3.40 (m, 1H), 3.28 (s, 3H), 1.74 (s, 3H). HRMS (ESI): Calculated for $\text{C}_{30}\text{H}_{34}\text{O}_7$ $[\text{M}+\text{Na}]^+$ 529.2197, found 529.2195.

Synthesis of Compound 4: To a stirring solution of **3** (5 g, 9.87 mmol) and benzyl *N*-(5-hydroxypentyl)carbamate (23.42 g, 98.7 mmol) in dry DCM (100 mL), $\text{BF}_3 \cdot \text{Et}_2\text{O}$ (1.22 mL, 9.87 mmol) was added in the presence of activated 4 Å molecular sieves at rt, and the reaction mixture was stirred for 2 h. After completion of the reaction as monitored by TLC, the reaction mixture was diluted with DCM and filtered through the pad of celite. The filtrate was washed with saturated sodium bicarbonate and brine, dried over anhydrous Na_2SO_4 , and concentrated to yield the acetoxy derivative which was used further without purification. Acetoxy derivative (7 g, 9.87 mmol) was taken in dry MeOH (200 mL) and to it 25 wt% sodium methoxide (700 μL) was added. The reaction was stirred at rt for 4 h. Neutralized with Dowex 50WX8 (H^+) resin, filtered, washed with methanol, and concentrated under reduced pressure. The obtained crude product was purified by column chromatography using hexane/ethyl acetate to yield the desired product **4** (5.48 g, 83%). $^1\text{H NMR}$ (500 MHz, CDCl_3): δ 7.40–7.20 (m, 20H), 5.12 (s, 2H), 4.91 (s, 1H), 4.85 (d, 1H, $J = 10.8$ Hz), 4.76–4.66 (m, 3H), 4.58–4.53 (m, 2H), 4.05 (s, 1H), 3.92–3.85 (m, 2H), 3.81–3.68 (m, 4H), 3.46–3.41 (m, 1H), 3.21–3.18 (m, 2H), 2.31 (brs, 1H), 1.61–1.51 (m, 4H), 1.39–1.34 (m, 2H); $^{13}\text{C NMR}$ (125 MHz, CDCl_3): 156.50, 138.37, 138.08, 136.76, 128.62, 128.47, 128.40, 128.19, 128.10, 128.01, 127.94, 127.93, 127.81, 127.67, 99.30, 80.40, 75.28, 74.48, 73.57, 72.08, 71.21, 69.15, 68.52, 67.56, 66.71, 41.09, 29.83, 29.13, 23.48. HRMS (ESI): Calculated for $\text{C}_{40}\text{H}_{47}\text{NO}_8$ $[\text{M}+\text{Na}]^+$ 692.3194, found 692.3192.

Synthesis of Compound Man-NH₂: To a stirring solution of **4** (3 g, 4.48 mmol) in dry methanol (50 mL), 25 wt% sodium methoxide (500 μL) was added at rt and the reaction mixture was stirred for 2 h. After completion of the reaction as monitored by TLC, the reaction mixture was neutralized with Dowex 50WX8 (H^+) resin, filtered, washed with methanol, and concentrated under reduced pressure. The obtained crude product was dissolved in a mixture of $\text{CF}_3\text{CH}_2\text{OH}$ and H_2O (9:1, 60 mL) with 1% HCOOH and to it, Pd/C (10%, 1 g) was added. The reaction mixture was stirred under an H_2 atmosphere for 24 h. The reaction mixture was filtered through a pad of celite, washed with methanol/water (4:1), concentrated, re-dissolved in water, and freeze-dried to yield the desired product Man-NH₂ (0.9 g, 76%). $^1\text{H NMR}$ (500 MHz, CD_3OD): δ 4.76 (s, 1H), 3.85 (dd, 1H, $J = 11.8, 2$ Hz), 3.80 (dd, 1H, $J = 3.2, 1.6$ Hz), 3.78 (dt, 1H, $J = 9.8, 6.6$ Hz), 3.72 (dd, 1H, $J = 11.2, 5.2$ Hz), 3.70 (dd, 1H, $J = 9.6, 3.9$ Hz), 3.61 (t, 1H, 9.5 Hz), 3.54 (ddd, 1H, $J = 9.7, 6, 1.9$ Hz), 3.45 (dt, 1H, $J = 9.8, 6.1$ Hz), 2.70 (t, 2H, $J = 7.3$ Hz), 1.63 (dq, 4H, $J = 13.5, 6.6, 6.6$ Hz), 1.45 (quin, 2H, $J = 6.9$ Hz); $^{13}\text{C NMR}$ (125 MHz, CD_3OD): 100.23, 73.37, 71.35, 70.82, 67.36, 66.80, 61.66, 39.69, 28.80, 27.99, 23.09. HRMS (ESI): Calculated for $\text{C}_{11}\text{H}_{23}\text{NO}_6$ $[\text{M}+\text{H}]^+$ 266.1598, found 266.1592.

Synthesis of Compound 5: Compound **4** (3 g, 4.48 mmol, 1 eq) and trichloroacetimidate derivative A (3.3 g, 6.72 mmol, 1.5 eq) were first dehydrated via co-evaporating with toluene and then dried under high vacuum for 2 h. The dried mixture was dissolved in dry DCM (100 mL), treated with activated 4 Å molecular sieves, and cooled to -20°C . TMSOTf solution (150 μL) was added and allowed to stir at rt for 1 h. After stirring for 1 h, the reaction was quenched with triethylamine, filtered through a pad of celite, and concentrated under reduced pressure. The obtained crude product was purified by column chromatography using hexane/ethyl acetate to yield the desired disaccharide **5** (3.5 g, 78%). $^1\text{H NMR}$ (500 MHz, CDCl_3): δ 7.40–7.27 (m, 18H), 7.21–7.19 (m, 2H), 5.49 (dd, 1H, $J = 3.4, 1.8$ Hz), 5.45 (dd, 1H, $J = 9.9, 3.4$ Hz), 5.29 (t, 1H, $J = 10.0$ Hz), 5.11 (s, 2H), 5.02 (dd, 1H, $J = 1.6$ Hz), 4.90 (dd, 1H, $J = 1.6$ Hz), 4.85 (d, 1H, $J = 10.9$ Hz), 4.75 (d, 1H, $J = 11.8$ Hz), 4.67–4.53 (m, 4H), 4.28 (dd, 1H, $J = 12, 5.2$ Hz), 4.24–4.21 (m, 1H), 4.14 (dd, 1H, $J = 12, 2.1$ Hz), 3.96–3.88 (m, 3H), 3.80–3.69 (m, 4H), 3.41 (dt, 1H, $J = 9.3, 6.3$ Hz), 3.19 (dd, 2H, $J = 12.8, 6.4$ Hz), 2.13 (s, 3H), 2.11 (s, 3H), 2.03 (s, 3H), 2.02 (s, 3H), 1.60 (quin, 2H, $J = 7.0$ Hz), 1.52 (quin, 2H, $J = 7.2$ Hz), 1.39–1.33 (m, 2H), 1.30 (brs, 1H); $^{13}\text{C NMR}$ (125 MHz, CDCl_3): 170.65, 169.88, 169.77, 169.71, 156.44, 138.43, 138.34, 138.28, 136.71, 128.55, 128.44,

128.40, 128.37, 128.22, 128.12, 127.73, 127.70, 127.62, 127.51, 127.47, 99.36, 98.58, 79.61, 76.42, 75.35, 74.90, 73.25, 72.41, 71.87, 69.51, 69.25, 69.14, 69.88, 67.61, 66.62, 66.31, 62.66, 40.97, 29.76, 29.14, 23.43, 20.93, 20.79, 20.76, 20.71. HRMS (ESI): Calculated for $\text{C}_{54}\text{H}_{65}\text{NO}_{17}$ $[\text{M}+\text{Na}]^+$ 1022.4145, found 1022.4221.

Synthesis of Compound Mana1,2Man-NH₂: To a stirring solution of **5** (3 g, 3 mmol) in dry methanol (50 mL), 25 wt% sodium methoxide (500 μL) was added at rt and the reaction mixture was stirred for 2 h. After completion of the reaction as monitored by TLC, the reaction mixture was neutralized with Dowex 50WX8 (H^+) resin, filtered, washed with methanol, and concentrated under reduced pressure. The obtained crude product was dissolved in a mixture of $\text{CF}_3\text{CH}_2\text{OH}$ and H_2O (9:1, 60 mL) with 1% HCOOH and to it, Pd/C (10%, 1 g) was added. The reaction mixture was stirred under an H_2 atmosphere for 24 h. The reaction mixture was filtered through a pad of celite, washed with methanol/water (4:1), concentrated, re-dissolved in water, and freeze-dried to yield the desired product Mana1,2Man-NH₂ (1 g, 79%). $^1\text{H NMR}$ (500 MHz, D_2O): δ 4.96 (d, 1H, $J = 1.2$ Hz), 4.88 (d, 1H, $J = 1.2$ Hz), 3.93 (dd, 1H, $J = 3, 1.2$ Hz), 3.81 (dd, 1H, $J = 3, 1.2$ Hz), 3.76 (m, 1H), 3.74–3.73 (m, 2H), 3.70 (dd, 1H, $J = 9.6, 3.3$ Hz), 3.64–3.37 (m, 8H), 2.77 (t, 2H, $J = 7.5$ Hz), 1.55–1.46 (m, 4H), 1.33–1.26 (m, 2H); $^{13}\text{C NMR}$ (125 MHz, D_2O): 156.50, 138.37, 138.07, 136.75, 128.62, 128.47, 128.40, 128.18, 128.10, 128.00, 127.94, 127.93, 127.80, 127.67, 99.29, 80.39, 75.27, 74.47, 73.56, 72.07, 71.20, 69.15, 68.51, 67.55, 66.71, 41.09, 29.83, 29.12, 23.48. HRMS (ESI): Calculated for $\text{C}_{17}\text{H}_{33}\text{NO}_{11}$ $[\text{M}+\text{H}]^+$ 428.2126, found 428.2109.

Preparation of Multivalent LPG₄₀Man_{0.60} and LPG₄₀(Mana1,2Man)_{0.60}: The multivalent mannosides (LPG₄₀Man_{0.60} and LPG₄₀(Mana1,2Man)_{0.60}) with 60% degree of functionalization were obtained in multiple steps starting from LPG₄₀OH as shown in Scheme 2.

Synthesis of LPG₄₀Alkyne_{0.60}: Dried LPG₄₀OH (588 mg, 7.95 mmol per monomer unit), as prepared (Mn: 43 kDa, PDI = 1.2, see GPC in ESI, Figure S21, Supporting Information) by the already reported procedure,^[30,31] was dissolved in dry DMF (30 mL) and placed in an ice bath at 0°C . Then 60% NaH (381 mg, 2 eq per OH to be functionalized) was added followed by dropwise addition of 80% propargyl bromide (640 μL , 1.2 eq per OH to be functionalized) and stirred at rt for 24 h. After that, the reaction was quenched with a small amount of water, and the resulting mixture was concentrated at reduced pressure. The crude obtained was dialyzed in MeOH for 2 days to afford colorless viscous in 68% yield. $^1\text{H NMR}$ (500 MHz, CDCl_3): δ 4.17 (s, 1.2H, alkyne methylene protons), 3.65 (brs, 5H, LPG backbone), 2.49 (s, 0.6H, alkyne terminal proton). M_n (NMR analysis) $\approx 51\,000$ g mol⁻¹.

Synthesis of LPG₄₀Acid_{0.60}: LPG₄₀Alkyne_{0.60} (DF = 0.60) (100 mg, 1.03 mmol per alkyne groups to be functionalized) and ethyl 3-azidopropanoate (177 mg, 1.2 eq per alkyne to be functionalized) were taken in 100 mL round bottom flask together with 30 mL of DMF. $\text{CuSO}_4 \cdot 5\text{H}_2\text{O}$ (51 mg, 0.2 eq per alkyne to be functionalized) and sodium ascorbate (204 mg, 1 eq per alkyne to be functionalized) were dissolved separately in a minimum amount of water and mixed well to form a yellow-colored adduct. The formed adduct was added to the mixture of LPG₄₀Alkyne_{0.60} and ethyl 3-azidopropanoate in DMF and stirred at 50°C for 24 h. After 24 h, the solvent was evaporated, and the residue was mixed with 5 mL of 2 N aq. NaOH and again stirred for 3 h at rt. The reaction mixture was then neutralized with 1 N HCl and dialyzed against water and EDTA for 3 days while changing the solvent thrice a day. The dialyzed product was then freeze-dried to yield the purified product at 78% yield. $^1\text{H NMR}$ (500 MHz, CDCl_3): δ 8.03 (s, 0.6H, triazole), 4.64 (s, 1.2H), 3.71 (brs, 6.2H, LPG backbone and methylene group), 2.79 (s, 1.2H). M_n (NMR analysis) $\approx 89\,000$ g mol⁻¹.

Synthesis of LPG₄₀Man_{0.60}: To a stirred solution of LPG₄₀Acid_{0.60} (DF = 0.60) (100 mg, 0.60 mmol per acid group to be functionalized) in DMF:H₂O (6:4, 30 mL), EDC.HCl (173 mg, 1.5 eq), HOBT (81 mg, 1 eq), and DIPEA (155 mg, 2 eq) were added at 0°C . The reaction mixture was stirred for 30 min followed by the addition of Man-NH₂ (239 mg, 1.5 eq per acid group to be functionalized). The resultant mixture was allowed to react at 50°C for 48 h. After 48 h, the solvent was evaporated, and the residue obtained was dialyzed against water for 3 days while changing the solvent thrice a day. The dialyzed product was then freeze-dried to yield

the purified product with an 81% yield. ^1H NMR (500 MHz, CDCl_3): δ 8.14 (brs, 0.04H, triazole), 3.92–3.66 (m, 1H), 3.33–3.06 (m, 0.23H), 2.89 (s, 0.23H), 2.04–1.93 (m, 0.05H), 1.65–1.10 (m, 0.20H, aliphatic chain). M_n (NMR analysis) \approx 169 000 g mol^{-1} .

Synthesis of $\text{LPG}_{40}(\text{Man}\alpha 1,2\text{Man})_{0.60}$: To a stirred solution of $\text{LPG}_{40}\text{Acid}_{0.60}$ (DF = 0.60) (100 mg, 0.60 mmol acid group to be functionalized) in $\text{DMF}:\text{H}_2\text{O}$ (6:4, 30 mL), EDC.HCl (173 mg, 1.5 eq), HOBT (81 mg, 1 eq), and DIPEA (155 mg, 2 eq) were added at 0°C . The reaction mixture was stirred for 30 min followed by the addition of $\text{Man}\alpha 1,2\text{Man-NH}_2$ (385 mg, 1.5 eq per acid group to be functionalized). The resultant mixture was allowed to react at 50°C for 48 h. After 48 h, the solvent was evaporated, and the residue obtained was dialyzed against water for 3 days while changing the solvent thrice a day. The dialyzed product was then freeze-dried to yield the purified product with 85% yield. ^1H NMR (500 MHz, CDCl_3): δ 8.18 (brs, 0.07H, triazole), 5.12–5.05 (m, 0.14H), 4.10–3.65 (m, 1H), 3.24–3.03 (m, 0.15H), 2.91 (s, 0.16H), 2.05–1.99 (m, 0.08H), 1.68–1.11 (m, 0.30H, aliphatic chain). M_n (NMR analysis) \approx 221 000 g mol^{-1} .

Supporting Information

Supporting Information is available from the Wiley Online Library or from the author.

Acknowledgements

N.H. and B.P. contributed equally to this work. This work is supported by funding from the Deutsche Forschungsgemeinschaft (DFG) – Projektnummer 458564133.

Open access funding enabled and organized by Projekt DEAL.

Conflict of Interest

The authors declare no conflict of interest.

Data Availability Statement

The data that support the findings of this study are available in the supplementary material of this article.

Keywords

adhesion inhibition, *Escherichia coli*, glycopolymers, microscale thermophoresis, poly(Man α 1,2Man), polyMan

Received: September 18, 2023

Revised: October 27, 2023

Published online:

- [1] V. S. Braz, K. Melchior, C. G. Moreira, *Front. Cell. Infect. Microbiol.* **2020**, *10*, 548492.
- [2] J. Jang, H.-G. Hur, M. J. Sadowsky, M. N. Byappanahalli, T. Yan, S. Ishii, *J. Appl. Microbiol.* **2017**, *123*, 570.
- [3] J. B. Kaper, J. P. Nataro, H. L. T. Mobley, *Nat. Rev. Microbiol.* **2004**, *2*, 123.
- [4] I. C. A. Scaletsky, S. H. Fabbriotti, R. L. B. Carvalho, C. R. Nunes, H. S. Maranhão, M. B. Morais, U. Fagundes-Neto, *J. Clin. Microbiol.* **2002**, *40*, 645.

- [5] R. M. Robins-Browne, A.-M. Bordun, M. Tauschek, V. R. Bennett-Wood, J. Russell, F. Oppedisano, N. A. Lister, K. A. Bettelheim, C. K. Fairley, M. I. Sinclair, M. E. Hellard, *Emerging Infect. Dis.* **2004**, *10*, 1797.
- [6] A. P. Daga, V. L. Koga, J. G. M. Soncini, C. M. De Matos, M. R. E. Perugini, M. Pelissou, R. K. T. Kobayashi, E. C. Vespero, *Front. Cell. Infect. Microbiol.* **2019**, *9*, 191.
- [7] B. Foxman, *Infect. Dis. Clin. North Am.* **2014**, *28*, 1.
- [8] X.-R. Wu, T.-T. Sun, J. J. Medina, *Cell Biol.* **1996**, *93*, 9630.
- [9] C.-S. Hung, J. Bouckaert, D. Hung, J. Pinkner, C. Widberg, A. Defusco, C. G. Auguste, R. Strouse, S. Langermann, G. Waksman, S. J. Hultgren, *Mol. Microbiol.* **2002**, *44*, 903.
- [10] I. Jorgensen, P. C. Seed, *PLoS Pathog.* **2012**, *8*, e1002907.
- [11] N. M. Poole, S. I. Green, A. Rajan, L. E. Vela, X.-L. Zeng, M. K. Estes, A. W. Maresso, *Infect. Immun.* **2017**, *85*, e00581.
- [12] A. Mittal, Krishna, Aarti, S. Prasad, P. K. Mishra, S. K. Sharma, B. Parshad, *Mater. Adv.* **2021**, *2*, 3459.
- [13] M. Touaibia, A. Wellens, T. C. Shiao, Q. Wang, S. Sirois, J. Bouckaert, R. Roy, *ChemMedChem* **2007**, *2*, 1190.
- [14] N. Nagahori, R. T. Lee, S.-I. Nishimura, D. Pagé, R. Roy, Y. C. Lee, *ChemBioChem* **2002**, *3*, 836.
- [15] S. Ehrmann, C.-W. Chu, S. Kumari, K. Silberreis, C. Böttcher, J. Dervede, B. J. Ravoo, R. Haag, *J. Mater. Chem. B* **2018**, *6*, 4216.
- [16] T. Dumych, C. Bridot, S. Gouin, M. Lensink, S. Paryzhak, S. Szunerits, R. Blosssey, R. Bilyy, J. Bouckaert, E.-M. Krammer, *Molecules* **2018**, *23*, 2794.
- [17] S. Bhatia, D. Lauster, M. Bardua, K. Ludwig, S. Angioletti-Uberti, N. Popp, U. Hoffmann, F. Paulus, M. Budt, M. Stadtmüller, T. Wolff, A. Hamann, C. Böttcher, A. Herrmann, R. Haag, *Biomaterials* **2017**, *138*, 22.
- [18] M. K. Patel, B. Vijaykrishnan, J. R. Koeppel, J. M. Chalker, K. J. Doores, B. G. Davis, *Chem. Commun.* **2010**, *46*, 9119.
- [19] V. Gannedi, A. Ali, P. P. Singh, R. A. Vishwakarma, *Tetrahedron Lett.* **2014**, *55*, 2945.
- [20] I. Papp, J. Dervede, S. Enders, S. B. Riese, T. C. Shiao, R. Roy, R. Haag, *ChemBioChem* **2011**, *12*, 1075.
- [21] C. R. Becer, M. I. Gibson, J. Geng, R. Ilyas, R. Wallis, D. A. Mitchell, D. M. Haddleton, *J. Am. Chem. Soc.* **2010**, *132*, 15130.
- [22] M. N. Stadtmueller, S. Bhatia, P. Kiran, M. Hilsch, V. Reiter-Scherer, L. Adam, B. Parshad, M. Budt, S. Klenk, K. Sellrie, D. Lauster, P. H. Seeberger, C. P. R. Hackenberger, A. Herrmann, R. Haag, T. Wolff, *J. Med. Chem.* **2021**, *64*, 12774.
- [23] B. Parshad, M. N. Schlecht, M. Baumgardt, K. Ludwig, C. Nie, A. Rimondi, K. Hönzke, S. Angioletti-Uberti, V. Khatir, P. Schneider, A. Herrmann, R. Haag, A. C. Hocke, T. Wolff, S. Bhatia, *Nano Lett.* **2023**, *23*, 4844.
- [24] S. Duhr, D. Braun, *Proc. Natl. Acad. Sci. USA* **2006**, *103*, 19678.
- [25] S. A. I. Seidel, C. J. Wienken, S. Geissler, M. Jerabek-Willemsen, S. Duhr, A. Reiter, D. Trauner, D. Braun, P. Baaske, *Angew. Chem., Int. Ed.* **2012**, *51*, 10656.
- [26] A. Wellens, M. Lahmann, M. Touaibia, J. Vaucher, S. Oscarson, R. Roy, H. Remaut, J. Bouckaert, *Biochemistry* **2012**, *51*, 4790.
- [27] P. W. Russell, P. E. Orndorff, *J. Bacteriol.* **1992**, *174*, 5923.
- [28] C. Fessele, T. Lindhorst, *Biology* **2013**, *2*, 1135.
- [29] M. Hartmann, H. Papavlassopoulos, V. Chandrasekaran, C. Grabosch, F. Beiroth, T. K. Lindhorst, C. Röhl, *FEBS Lett.* **2012**, *586*, 1459.
- [30] P. Pouyan, C. Nie, S. Bhatia, S. Wedepohl, K. Achazi, N. Osterrieder, R. Haag, *Biomacromolecules* **2021**, *22*, 1545.
- [31] M. Tully, M. Dimde, C. Weise, P. Pouyan, K. Licha, M. Schirner, R. Haag, *Biomacromolecules* **2021**, *22*, 1406.